Rodney D. Brown III

New Methods for De Haas-Shubnikov Measurements

Abstract: Improved techniques and instrumentation for observing the de Haas-Shubnikov (dHS) effect are described and preliminary results of their application to measurements on bismuth are presented. The two main features of the method are: first, the monotonic H^2 term in the magnetoresistance is subtracted out, allowing increased amplification of the oscillatory part, and therefore increased sensitivity in detecting the periods; second, the magnetic field is swept such that $1/H$ varies linearly in time, producing dHS oscillations sinusoidal in time, making it possible to use real-time differentiation and filtering to separate interfering periods. The method thus provides a large amount of data reduction prior to recording, permits direct measurement and averaging of the periods from the recorded data, and allows a more accurate and unambiguous interpretation of the data. Much of the instrumentation described ($1/H$ sweep, filter, differentiator) has been built around commercially available operational amplifiers.

Introduction

• *The de Haas-Shubnikov effect*

Phenomenologically, the resistance of a metal or semimetal as a function of magnetic field (H) can be described by a constant term plus monotonically increasing terms of even powers of the magnetic field plus oscillatory terms which are periodic in $1/H$. These last terms are known as the dHS effect[1] and are normally observable only at liquid helium temperatures. The periods of the dHS oscillations provide a measure of various cross sections of the Fermi surface.[2] Often, only monotonic terms to order H^2 are observed up to fairly large fields. For a given material the amplitudes and signs of the various terms depend on the orientation of the magnetic field and current with respect to each other and to the crystallographic directions of the sample, and on the temperature. A material such as bismuth with a relatively simple Fermi surface can have a quite complicated magnetoresistance because of the superposition of the monotonic terms and oscillatory terms of different periods, the amplitudes of the latter terms usually being much smaller than those of the former.

This paper will describe experimental details of a new method for observing the transverse dHS effect and will give some preliminary results for bismuth.

• *General description of the method*[3]

Figure 1 shows a block diagram of the apparatus. The H^2 term in the magnetoresistance is eliminated as follows. There are two samples of the material under study, one at the temperature of liquid nitrogen (labeled "bucking") where there are no magnetoresistance oscillations, and the other in liquid helium (labeled dHS), in which the oscillations are to be observed. The two samples are located in cryostats in the same magnetic field and supplied with constant currents from a common source. The relative sizes of the samples are chosen such that for reasonable values of current, i.e., values at which the self-field in the dHS sample and heating effects in the bucking sample are negligible, the H^2-dependent part of the voltage across the bucking sample can be made equal to the H^2-dependent part of the voltage across the dHS sample. The difference between the voltages across the two samples is taken in the bridge, the output of which is proportional to the oscillatory part of the magnetoresistance of the dHS sample. A small voltage due to deviation from strictly quadratic field dependence of the monotonic part of the magnetoresistance of either of the samples is also present for some values of the magnetic field. The bridge output is fed through an amplifier, differentiator, or tunable low-frequency, low-Q filter, or combination of these to the Y axis of an X-Y recorder.

The quantity $1/H$ is varied linearly in time as follows: in the Hall Probe Field Control (HPFC) the output voltage of the Hall probe is compared to a fraction of the voltage generated by the $1/H$ sweep, the reciprocal of which varies linearly in time. The difference between these two voltages is fed to the null detector of the current regulator in the magnet power supply, causing the field to follow the $1/H$ sweep. The $1/H$ sweep also provides a linear drive for the X axis of the recorder, which is calibrated in reciprocal gauss.

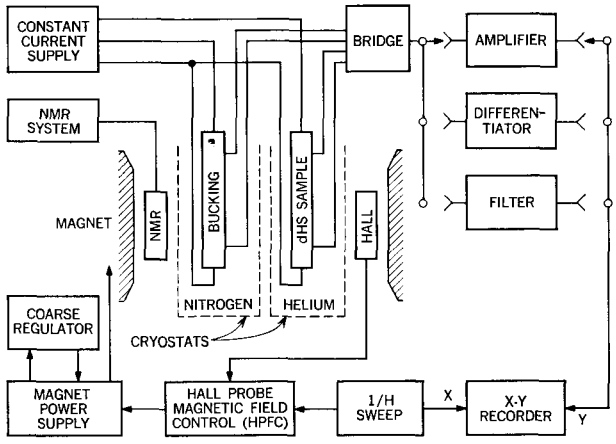

Figure 1 Block diagram of the apparatus.

Recording the data in this manner provides a large amount of data reduction compared to recording magnetoresistance as a function of magnetic field, where it is necessary to plot ordinal numbers of maxima or minima vs calculated values of $1/H$ to determine the periods. In this method the periods (in $1/H$) of the observed oscillation are determined by direct measurement on the recorder trace; averaging is accomplished by measuring over the span of a known number of periods.

Experimental details

- *Sample preparation*

Both the dHS and bucking samples were cut from large single crystals grown by a modified Bridgman technique from 99.999% pure, zone-refined bismuth. A melt of approximately 10 kg was contained in a pyrex beaker with gently tapered (~5°) sides and a sharply tapered (~45°) conical bottom that had been coated with carbon from an oxygen-poor gas flame, except for a small spot in the tip that was cleaned. The beaker was covered with a loose-fitting graphite lid that supported a disk heater and was contained in a vertical oven. The melt filled the beaker almost to the lid. The power to the oven was dropped to zero over a period of about 18 hours while a temperature gradient was maintained in the melt by the disk heater. It usually took three to six tries to grow a single crystal approximately three inches long and two inches in diameter. Between tries the charge was heavily etched with 35% nitric acid and the beaker was cleaned and recarboned. Neutron scattering data from crystals grown in this manner showed a high degree of perfection.[4] The crystals were oriented by cleaving and etching. The samples were cut and planed with a Servomet spark cutter and etched in 35% nitric acid. Two leads were attached to each end with Ceroseal 160 solder.

- *Cryostats and sample holders*

Two standard metal dewars, one for the nitrogen sample and one for the helium sample, are situated in the same magnetic field. Both sample holders provide for four-terminal resistance measurements and for rotation of the samples about an axis perpendicular to the magnetic field. The dHS sample holder was constructed so that the orientation of the sample with respect to the field was known to within 2° about the axis of rotation and approximately 0.5° along the axis of rotation. The final orientation of the sample about its axis of rotation was determined to within 0.5° by observing the magnetoresistance as a function of angle at 77°K (see Ref. 5). Relative angles could be measured to 0.1°. The bucking sample usually had the current and its long axis along the trigonal direction and the magnetic field in the trigonal plane. This sample was rotated for minimum noise, which corresponded to a maximum or minimum in the magnetoresistance. In order to eliminate noise presumably due to charged bubbles of nitrogen gas forming on the surface of the bucking sample at fairly high power inputs, the sample was enclosed in a grounded, hermetically sealed brass can filled with helium gas, the leads being brought out through standard glass-to-metal seals.

- *Sample sizes and currents; sensitivity*

The voltages (V) across the two samples shown in Fig. 1 are given by

$$V_d = \frac{L_d}{A_d}\left[\rho_d^{(0)}(T) + \rho_d^{(2)}(T)H^2 + \rho_d^{\mathrm{osc}}(T, H)\right]I_d$$
$$= V_d^{(0)} + V_d^{(2)} + V_d^{\mathrm{osc}} \qquad (1)$$

and

$$V_b = \frac{L_b}{A_b}\left[\rho_b^{(0)}(T) + \rho_b^{(2)}(T)H^2 + 0\right]I_b$$
$$= V_b^{(0)} + V_b^{(2)} + 0, \qquad (2)$$

where d and b refer to the dHS and bucking samples, respectively, L is the distance between potential contacts, A the cross-sectional area of the sample, $\rho^{(0)}$ the field independent term in the resistivity, $\rho^{(2)}$ the magnetoresistance (which is zero in the bucking sample at liquid nitrogen temperatures), I the sample current, H the magnetic field, which is the same for both samples, and T the temperature.

The ratio of the magnetoresistance coefficients $\rho_d^{(2)}/\rho_b^{(2)}$ can be as large as 100 (Ref. 6) depending on the purity and perfection of the samples and the relative directions of the currents and magnetic fields. For typical samples used in this experiment the ratio was of the order of 40 to 80. In order to operate with reasonable currents in both samples, the current in the dHS sample being limited to ~100 mA by self-field effects, the ratio of the cross-sectional areas of

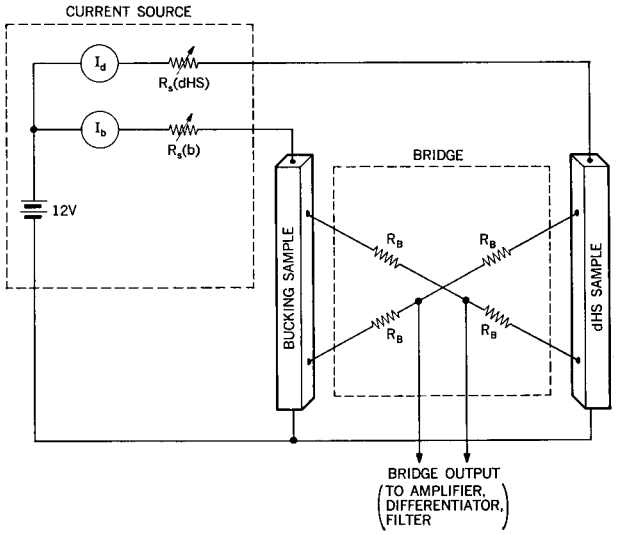

Figure 2 Schematic diagram of the current source and bridge.

the two samples A_d/A_b was adjusted to the same order of magnitude as $\rho_d^{(2)}/\rho_b^{(2)}$. Typical sample dimensions were 0.46 cm × 0.51 cm × 4.7 cm for the dHS sample and 0.05 cm × 0.1 cm × 4.0 cm for the bucking sample.

The above figures are only approximate for both samples due to the anistropy of $\rho^{(2)}$ with magnetic field. The dHS sample current was usually held constant, the bucking sample current being adjusted for optimum cancellation of the H^2 terms as the dHS sample was rotated in the magnetic field. Typical sample currents were $I_d = 40$ mA with I_b ranging from 35 to 80 mA, which gave sample voltages of approximately 30 to 50 mV at 10 kgauss. The oscillatory part detected ranged from 50% to 0.1% of the total voltage across the dHS sample. In these preliminary measurements, not too much attention was paid to absolute voltage levels, as long as the periods were observable. When the filter was used the exact gain of the system was not always known. The noise was of the order of 5 μV, with random drifts, under the worst conditions, of about 10 μV.

Instrumentation

- *Current source and bridge*

The essentials of the constant current source and the bridge circuit are shown in Fig. 2. The current source consists of a 12-V storage battery and variable current-limiting resistors which are large compared to the largest value of sample resistance. The latter is of the order of a few ohms.

The bridge resistors (R_B) have values of 2 kΩ, which is large compared to the largest sample resistance, but small compared to the input impedances of the amplifier, differentiator and filter, which are on the order of 10^6 ohms. This arrangement eliminates the voltage drop in the leads and across the end contacts of the samples (although for all the measurements presented below the potential leads were connected to the ends of the samples with no observable effect). From Eqs. (1) and (2), for optimum cancellation of the H^2 term, the output of the bridge (V_B) is given by

$$V_B = \frac{V_d^{(\mathrm{osc})} + V_d^{(0)} - V_b^{(0)}}{2}, \tag{3}$$

where $(V_d^{(0)} - V_b^{(0)})/2$ is constant and due mostly to $V_b^{(0)}$; at most fields this is negligible. Where it becomes significant it can be bucked out by adding the proper voltage in one of the arms or at the output of the bridge. The common voltage source and bridge arrangement cause noise in the source to be cancelled in the output of the bridge. The bridge also has a switching arrangement which allows measurement of the total voltage across each sample.

The current source, bridge and samples are floating and shielded, permitting one of the output points of the bridge to be grounded at the input of the amplifier, minimizing noise and pickup.

- *Detecting apparatus*

Amplifier

A Keithly micro-volt-ammeter, Model 150A, was used as an amplifier. The zero-suppress feature of this instrument was convenient for cancelling the constant voltage in the bridge output.

Figure 3 Schematic diagram and response of the differentiator.

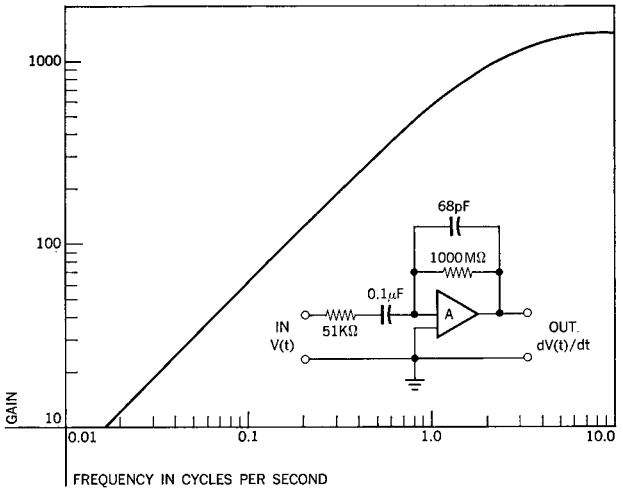

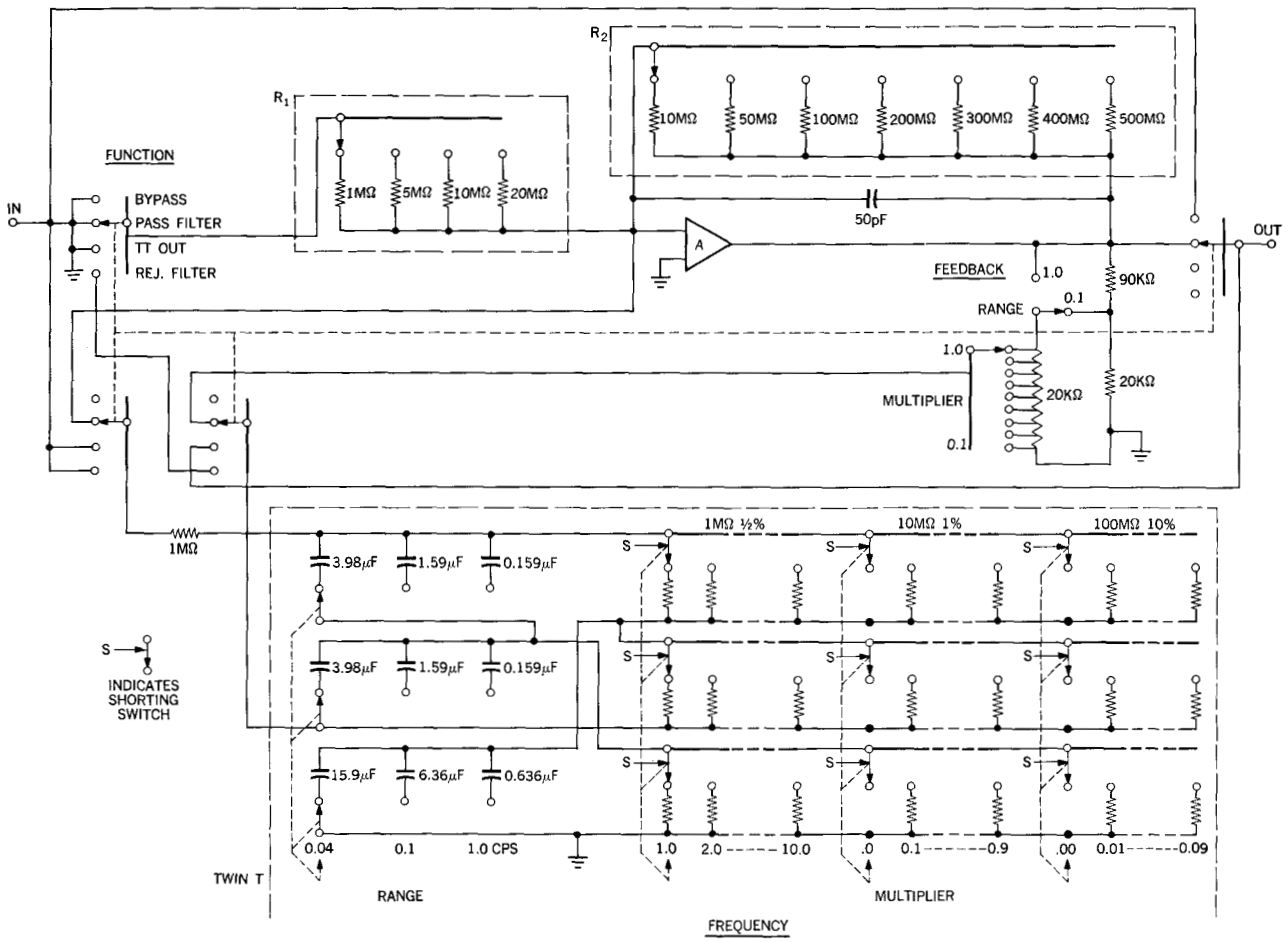

Figure 4 Schematic diagram of the low-frequency filter.

Differentiator

The differentiator, the schematic diagram and response of which is shown in Fig. 3, uses a high-gain operational amplifier (Philbrick USA-3) with capactive input and resistive feedback. The 68 pF capacitor and 51 kΩ resistor inhibit high-frequency oscillation.

Filter

The circuit for the tunable, variable-Q, low-frequency filter is shown in Fig. 4. This unit also employs a high-gain operational amplifier (USA-3) and a tunable Twin-T filter. The "T-T" can be switched to the feedback line, with resistive input, for a pass filter or to the input line, with resistive feedback for a rejection filter. It can also be switched to external jacks for use as a rejection filter with the differentiator for combined rejection and differentiation.

The T-T covers the range of frequencies from 0.04 to 10.99 Hz and is tuned as follows: Three ranges with minimum values of 0.04, 0.1, and 1 Hz are obtained by switching matched sets of fixed capacitors; multiplication by factors between 1.0 and 10.99 in steps of 0.01 is achieved by varying the elements of the three equal resistance arms, shown in Fig. 4. The 50 pF capacitor across the amplifier and the 1 MΩ resistor in series with the T-T were added to inhibit high- and low-frequency oscillation, respectively.

The effective Q in the pass mode can be adjusted either by varying the fraction of the output voltage fed back through the T-T, for which there are two 10-step FB ranges 1 to 0.1 and 0.1 to 0.01, or by varying the maximum gain, G, at resonance by adjusting the ratio of R_2 to $R_1 (G = R_2/R_1)$. The effective Q is given approximately by

$$Q = \text{FB} \times G \tag{4}$$

for R_1 large compared to the off-resonance impedance of the T-T and R_2 small compared to the on-resonance impedance. The effect of the first method is to keep the gain at the center frequency constant and to vary the gain on either side; the effect of the second method is to keep the gain at frequencies off resonance fairly constant and to vary the gain at the center frequency. The response of the

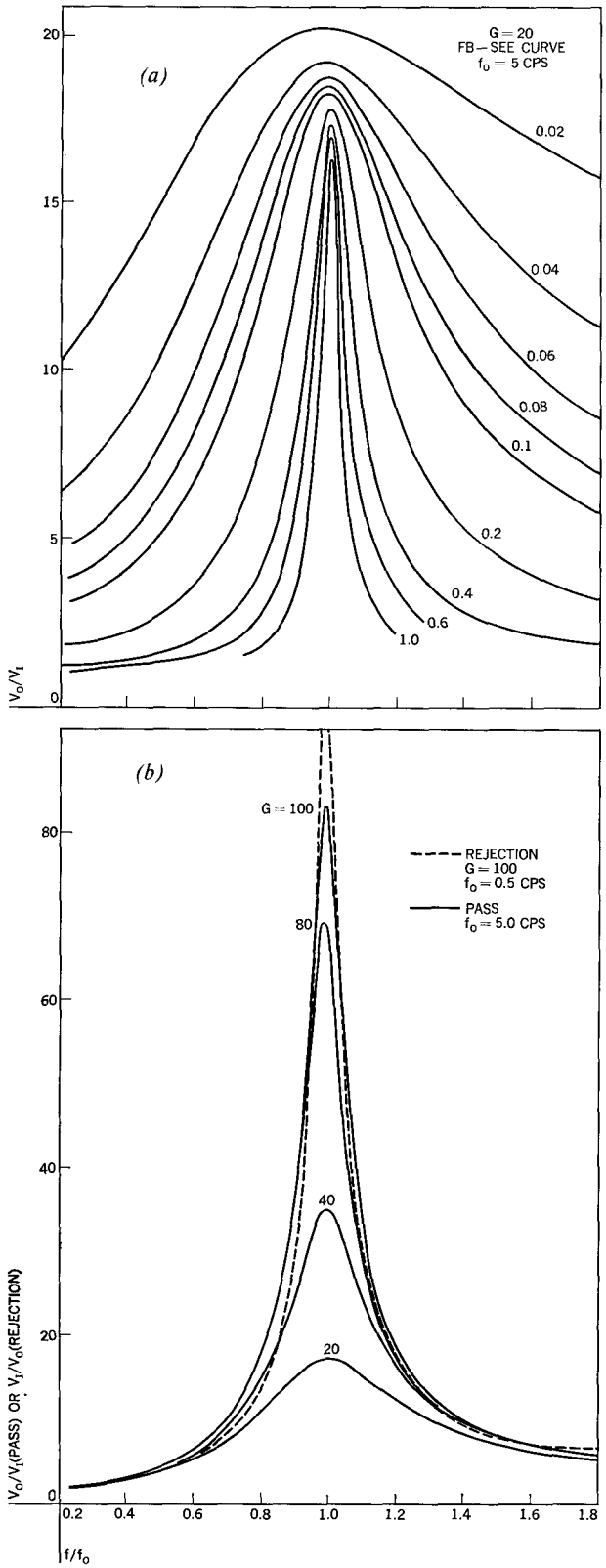

Figure 5 Filter response in the pass mode (a) for fixed gain and with feedback as a parameter; (b) for fixed feedback with gain as a parameter (solid curve) and filter response in the rejection mode (dashed curve).

filter between 1 and 10 Hz for the first type of variation, for $G = 20$, is shown in Fig. 5(a). The response for the second type of variation, for FB = 0.1, is shown in Fig. 5(b).

For rejection the T-T is in the input of the amplifier. The effective Q is adjusted by varying R_1 and R_2. The attenuation curve is shown in Fig. 5(b).

- *Magnetic field apparatus and sweep calibration*

The magnetic field apparatus consists of a 12-inch Varian electromagnet, Model V-4012, with a three-quarter inch gap, a modified Varian power supply, Model V-2100, a coarse regulator (CR), a Hall probe magnetic field control (HPFC) and a $1/H$ sweep generator. A nuclear magnetic resonance (NMR) system was used for calibrating the HPFC and for checking the magnetic field calibration during experimental runs.

Power supply modifications

The magnet power supply was modified by adding a position to the sweep selector switch in which the sweep input is fed directly into the null detector of the regulator chopper-amplifier. In this position the magnet supply reference battery, used for current regulation, is disconnected and the current sensing resistors are connected to the input of the chopper amplifier by a 0.5 μF capacitor so that the regulator will still be effective for removing ripple. An external control for field regulation can replace the reference source and sensing resistors used for current regulation.

Coarse regulator

For large field sweeps it is necessary to adjust the high voltage in the magnet power supply in order to keep the voltage across the pass tubes within their regulating range. The coarse regulator, which consists of a reference voltage, modified Brown chopper-amplifier and servo motor, does this by sensing the voltage at the regulating range meter of the magnet supply and servoing the autotransformer that feeds the high-voltage power supply.

Hall probe field control

The HPFC circuit is shown in Fig. 6. The probe consists of a Siemens FC-34 Hall element with the necessary circuitry to adjust for Hall arm offset and loading resistors to linearize the response of the probe.[7] The FC-34 has an output of approximately 20 mV/kgauss for an input current of 0.2 A. For manual control of the field, the constant voltage source which supplies the probe current through a resistor large with respect to the probe resistance also supplies a reference voltage across a 5 kΩ, 15 turn linear (0.05%) potentiometer. The output of the HPFC is the difference between the Hall probe output voltage and the voltage across part of the potentiometer. This is fed

into the sweep input of the magnet supply with the sweep input switch in the HPFC position. By adjusting the current through the potentiometer the manual dial can be calibrated directly in gauss. The use of a common voltage supply for the probe and reference minimizes changes in the HPFC output due to supply voltage changes. The output of the probe was linearized to within 0.5% or better by adjusting the linear matching resistor using NMR points between 3 and 10 kgauss.

In the sweep mode the probe output is compared to a fraction of an externally generated voltage fed into the sweep input of the HPFC.

In each mode (manual and sweep) the Hall element is operated with one Hall arm grounded. This allows one terminal of the probe voltage supply to operate with just a few ohms to ground and minimizes 60 Hz pickup. In operating the probe in this manner, the current which generates the reference voltage flows through the Hall element and its linearizing and offset resistors, generating a voltage which adds to the Hall voltage and which depends on the field through the magnetoresistance of the probe. However the maximum resistance through the probe arms is small compared to the resistance of the reference voltage generators, so that this effect is small except at very low fields.

The accuracy of the manual dial readings is at least 0.5% between approximately 3 and 10 kgauss and from the probe characteristics, at least 1% between 2 and 13.3 kgauss.

The noise at 10 kgauss as observed in a NMR signal was on the order of 2–3 gauss after about a one-hour warmup time. In the first hour the field drifts on the order

Figure 6 Schematic diagram of the Hall probe field control.

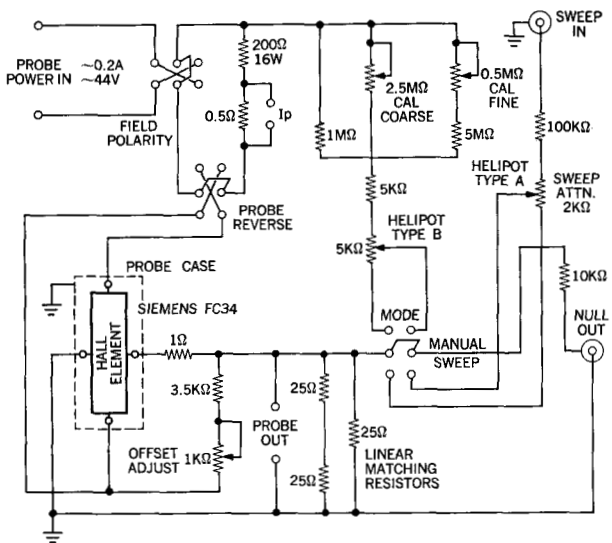

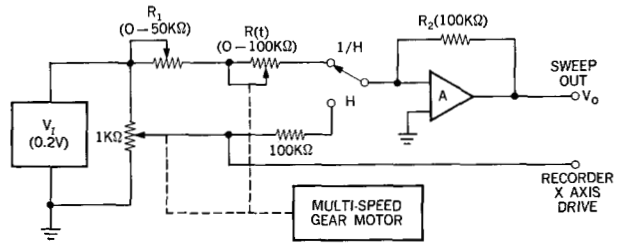

Figure 7 Schematic diagram of the reference voltage generator for sweeping either $1/H$ or H linearly in time.

of 10-20 gauss at 10 kgauss primarily due to changes in probe temperature. At the beginning of each run the practice was to calibrate at 10 kgauss and check at 5 kgauss using NMR. The dial reading at 5 kgauss always fell in the range 4980 to 4990.

An accuracy of 0.5% was sufficient for the dHS measurements. Improvements in accuracy, noise and stability can probably be achieved by temperature compensation or stabilization of the probe and by using a more stable voltage supply for the probe and reference.

$1/H$ Sweep

The $1/H$ sweep circuit is shown schematically in Fig. 7. A voltage, the reciprocal of which varies linearly with time, is generated by feeding an operational amplifier from a constant voltage source (V_I) and sweeping part of its input resistance $[R_1 + R(T)]$ linearly in time. The output voltage (V_o) is given by

$$1/V_o = (1/R_2 V_1)[R_1 + R(t)] = A + Bt, \qquad (5)$$

since the amplifier input currents must sum to zero. Thus, for fixed V_I and R_2, R_1 determines the starting voltage and $R(t)$ determines the variation of V_o with time.

The variable resistor (10-turn Helipot, Type A) is driven by a reversible synchronous motor through a multispeed gear box which provides total sweep times (10 turns of the potentiometer) of 20, 40, 80, 160, 320, and 640 sec in each direction. The output of the $1/H$ sweep is fed into the sweep input of the HPFC, the sweep range being determined by the sweep input attenuator. A potentiometer is ganged with $R(t)$ and is fed by the same constant voltage that feeds the $1/H$ sweep generator. The output of the potentiometer provides the linear drive for the X axis of the recorder.

The maximum sweep rate is limited chiefly by the time constant of the magnet, by heating effects in the sample and holder and by the range of periods to be measured and the response time of the detecting equipment. In practice, a convenient time for sweeping over the full range of field is chosen, and V_I and the X scale on the recorder are selected to give a convenient recorder deflection per second. Then,

using proton resonance points at 5 and 10 kgauss (2×10^{-4} and 1×10^{-4} gauss^{-1}) the sweep input attenuator is adjusted to give a convenient number of reciprocal gauss per recorder division. The value of R_1 then determines the high-field limit of the sweep, the motor drive speed determines the sweep rate in gauss^{-1}/sec and the total sweep is set by the X scale chosen on the recorder.

Most runs are made at a sweep rate of 0.5×10^{-5} gauss^{-1}/sec with deflections of either 2.0×10^{-5} gauss^{-1}/cm covering the range ~13 kgauss to 1.3 kgauss for the longer periods or 0.4×10^{-5} gauss^{-1}/cm covering ~13 kgauss to ~4.5 kgauss to obtain more detail in the shorter periods at the higher fields.

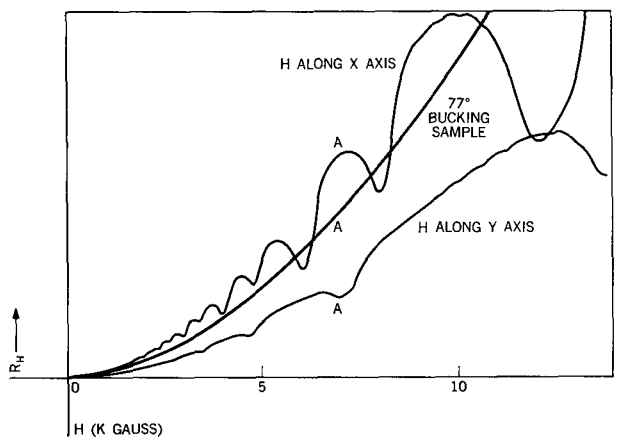

Figure 8 Magnetoresistance of a trigonal sample as a function of magnetic field (H) for H along the binary (X) and bisectrix (Y) direction and magnetoresistance of the bucking sample at 77°K.

At the above sweep rate, for periods between 0.5×10^{-5} gauss^{-1} and 10×10^{-5} gauss^{-1}, oscillation frequencies lie between about 0.05 and 1 Hz.

Experimental results

Examples of measurements of the transverse dHS effect made on bismuth crystals with the above apparatus and their interpretations are presented below. Three crystals, with current along the binary (X), bisectrix (Y), and trigonal (Z) axes and the magnetic field in the respective planes were used. Most measurements were made near 1.4°K at fields from 0.5 to 13.3 kgauss. In the Figures, A, D, F_P and F_R indicate the use of the amplifier, differentiator and pass or rejection filter, respectively, in taking the data. The period to which the filter is tuned is indicated in parentheses in units of 10^{-5} gauss^{-1}.

Figure 8 shows the total magnetoresistance of a trigonal sample for magnetic field along both the binary and bisectrix directions and the magnetoresistance of the bucking sample versus magnetic field.

Figure 9(a) shows only the oscillatory part of the magnetoresistance of the above sample versus $1/H$ for H in the Y direction for three amplifier gains. The long and short electron periods (8.05 and 4.05×10^{-5} gauss^{-1}) in this direction are readily determined by direct measurement on the graph. Figure 9(b) shows the high-field region of the previous curves on an expanded $1/H$ scale and the same region differentiated, from which the short hole period (0.48×10^{-5} gauss^{-1}) can be determined.

Figure 10(a) shows the oscillatory part of the magnetoresistance versus $1/H$ for H along X. The single long period (7.05×10^{-5} gauss^{-1}) is observed along with a short period near 10 kgauss. Figure 10(b) shows the 10

Figure 9(a) dHS oscillations in a trigonal sample for H along the bisectrix at three amplifier gains. (b) high-field region of (a) expanded and differentiated.

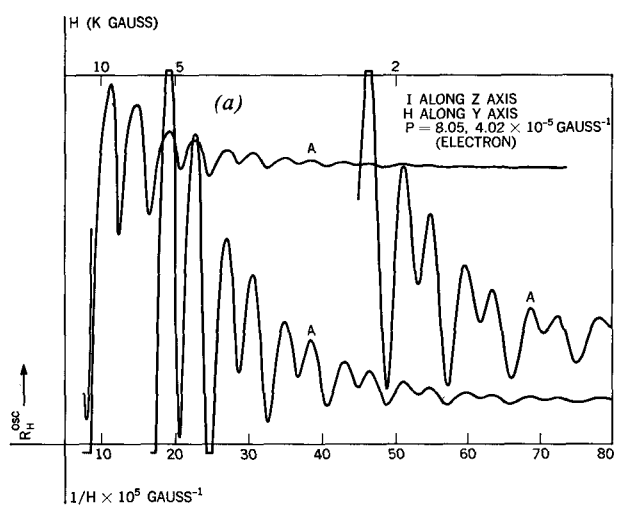

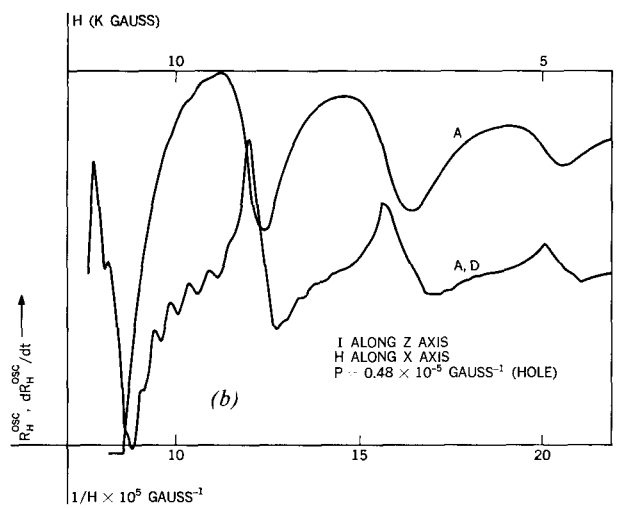

kgauss region expanded and differentiated. The short period (0.51×10^{-5} gauss^{-1}) is attributed to electrons.

Figures 8 to 10 show the data for the magnetic field directions in which each minimum can easily be associated with the correct period. Figure 11 shows data for the trigonal sample for the magnetic field 10° from the bisectrix at two amplifier gains. Here the oscillations are evident but the periods are not quite as obvious. It is in analyzing this type of data that this technique proves particularly useful. All of the minima can be accounted for if we start with the lower trace and label the obvious major minima by *a* and the minor ones by *b*. The *b* minima seem to be approximately splitting the maxima of the *a* component and to be slightly off being a multiple of the *a* period, since the splitting is shifting. In addition, there are two sharp minima on this trace which do not fit into either the *a* or *b* periods. If we label these minima *c*, and look further down in field, on the upper trace, we find minima with the same separation. Now if we reexamine the *a* and *b* minima we note that where they are unduly large they coincide with each other, with the *c* minima, or both. We find we have to supply the location of a few *a* and *b* minima at points where they are masked by other minima; however, when we do, we see three distinct electron periods of 2.81, 5.10, and 7.92×10^{-5} gauss^{-1}.

The above data illustrate the use of the bucking, $1/H$ sweep and differentiator in recording and analyzing data. The use of the filter and filter-differentiator combination is discussed below.

When operated in the pass mode, the filter is usually operated at low $Q(\sim 10)$ since the number of cycles observable is limited and since it can be shock-excited by long periods of large amplitude at high fields. To minimize the latter effect, the field was swept in the direction of increasing field. The effect of the filter for long periods is shown in Fig. 12(a), where it is used to separate the electron period at 4.1×10^{-5} gauss^{-1} from the one at 8.2×10^{-5} gauss^{-1} for H in the Y direction in a binary sample. The Q was 10 and the filter was tuned to periods of 4.16, 5.0, and 3.57×10^{-5} gauss^{-1}; in each case the period measured was 4.1×10^{-5} gauss^{-1} within experimental accuracy of $<1\%$.

The effect of the pass filter for shorter periods is shown in Fig. 12(b). For the above sample the hole period of $\sim 0.5 \times 10^{-5}$ gauss^{-1} is separated from the two electron periods. Traces are shown for no filter, and with the filter

Figure 10(a) dHS oscillations in a trigonal sample for H along the binary at two amplifier gains. (b) High-field region of (a) expanded and differentiated.

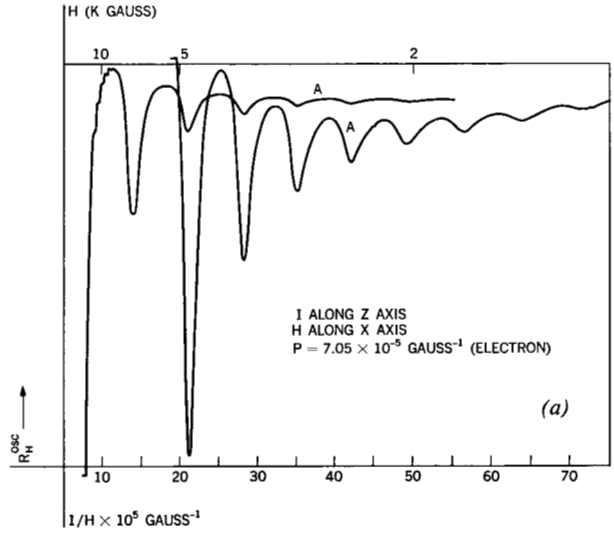

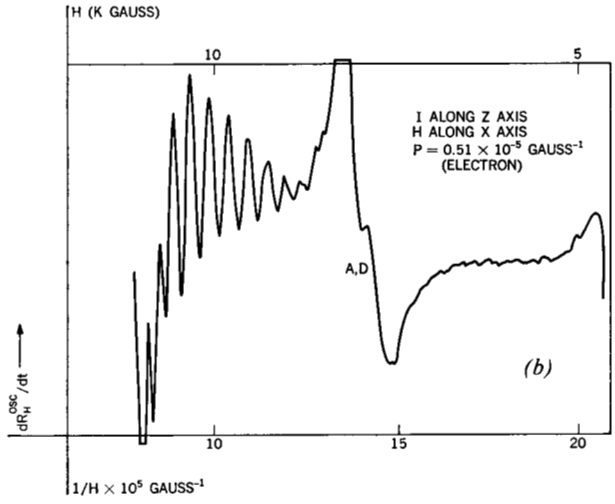

Figure 11 dHS oscillations in a trigonal sample for H at 10° from the bisectrix at two amplifier gains.

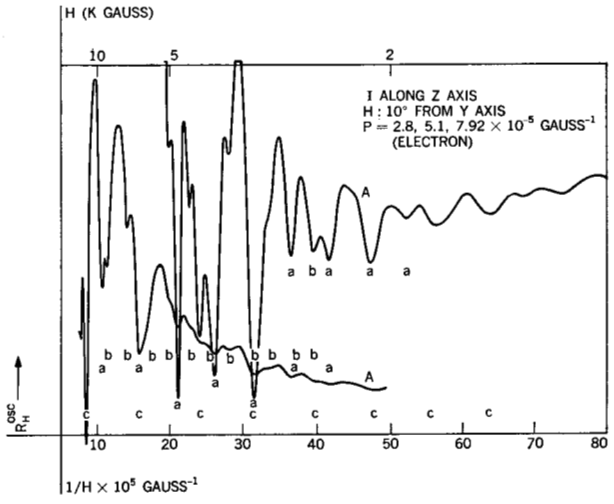

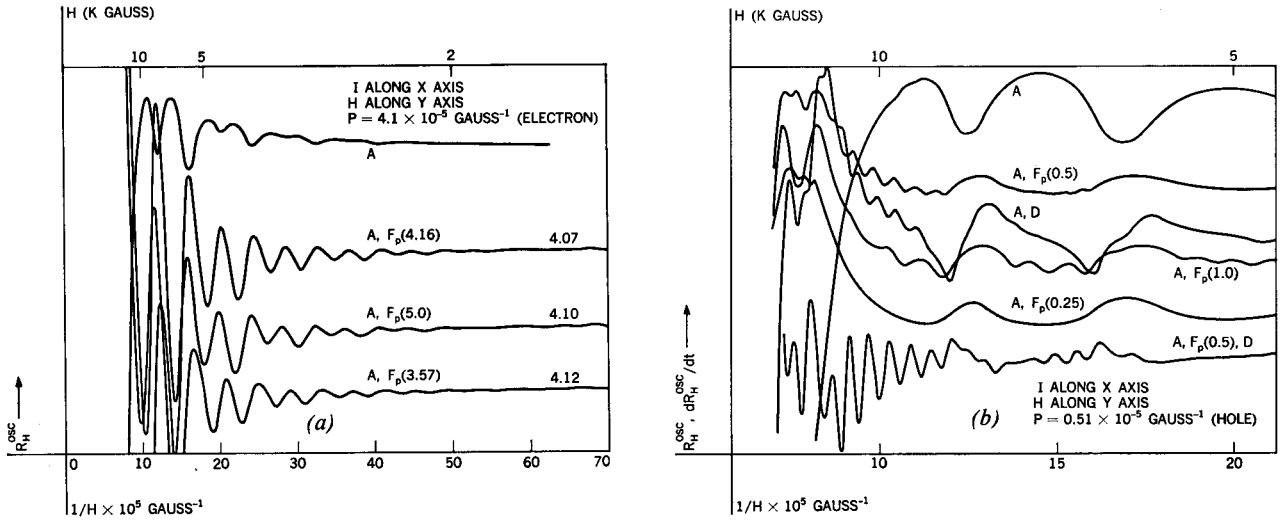

Figure 12(a) dHS oscillations in a binary sample for H along the bisectrix using the amplifier only and using the amplifier and pass filter tuned to three periods. (b) High-field region of (a) expanded, illustrating the effects of differentiating, pass filtering, and the combination of differentiating and pass filtering.

tuned to periods of 0.25, 0.5, and 1×10^{-5} gauss^{-1}. At 0.5 a period of 0.51×10^{-5} gauss^{-1} is found; hints of the same period when tuned to 0.25 are also seen. When tuned to 1.0, one or two cycles of this period are observed; however, these are due only to shock excitation by the large electron periods, which is seen from the fact that, although they occur early in the trace, they are correlated with the electron periods and each time a definite cycle is observed the amplitude decreases rather than increases with increasing field. Also shown for comparison is the differentiated trace.

The results obtained on using the differentiator after the filter for the same period are shown in the bottom trace, for which the Y-scale sensitivity is 1/10 that of the previous traces taken with the filter alone.

The use of the filter for rejection is illustrated in Fig. 13 for H $+14°$ from the trigonal of a binary sample. The major electron period can be determined from the unfiltered trace to be $\approx 2.98 \times 10^{-5}$ gauss^{-1}. Tuning the filter to reject this period shows up the hole period at 1.56×10^{-5} gauss^{-1}. Data with the filter tuned to reject the holes, which brings out the electron period more clearly, are shown in the middle trace.

An example of the combined use of the rejection filter and differentiator is shown in Fig. 14 for H at $-10°$ from the trigonal where the hole period of 1.56×10^{-5} gauss^{-1} is the dominant period observed. An attempt was made to observe the short electron period expected at this angle by rejecting the hole period and differentiating the filter output. However, the major period remaining was the second harmonic of the holes at $\approx 0.78 \times 10^{-5}$ gauss^{-1}, as confirmed by similar observation between $-24°$ and $+24°$. The electron period could not be observed in this direction.

Figure 13 dHS oscillations in a binary sample for H at $+14°$ from the trigonal using the filter to reject the electron period (2.98×10^{-5} gauss^{-1}) or the hole period (1.56×10^{-5} gauss^{-1}).

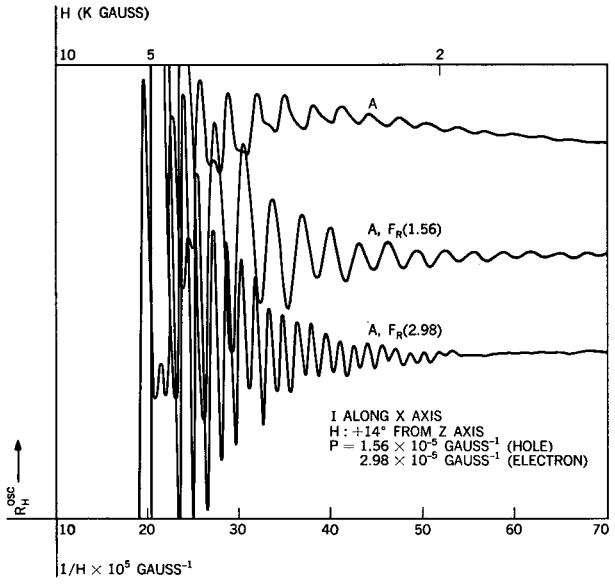

Discussion of results

The measured periods are known to accuracies ranging from $\sim 1\%$ to 10%. For well-defined periods the 1% limit is set by the field apparatus and sample orientation. The 10% limit is due to both a limited number of observable cycles and distortion by other periods.

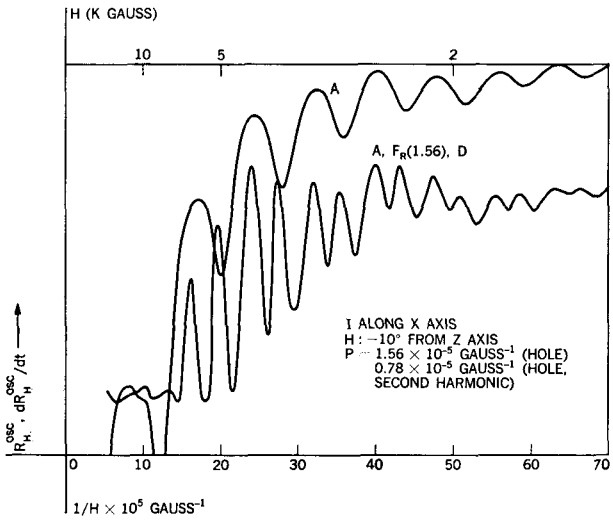

Figure 14 dHS oscillations in a binary sample for H at −10° from the trigonal using the T-T filter to reject the hole period at 1.56×10^{-5} gauss^{-1}, and the differentiator to bring out the expected short electron period. The short period actually observed is the second harmonic of the hole period.

For many directions of field in a given sample the periods observed are exact and unambiguous. However, for other directions the interpretation of data for one direction depends on data taken at adjacent directions, e.g., the short period found in Fig. 14 might have been mistaken for the electron period sought, or for a heavy carrier, without the data at adjacent angles which showed the correct magnitude and constant phase necessary for the hole period second harmonic.

Comparison with other methods

Some of the latest data on the dHS effect have been taken using a derivative technique.[8,9] In this method a small ac magnetic field is added to the dc field, producing a modulation in the voltage across the sample which is fed by a constant dc current. The ac component of the voltage is synchronously detected, rectified and plotted as a function of magnetic field. The trace is proportional to a derivative of the magnetoresistance with respect to the magnetic field (the particular derivative depending on the harmonic of the modulating frequency detected). Periods are found by plotting the ordinal numbers of the maxima or minima versus calculated value of $1/H$.

The present method includes all the advantages of the derivative technique plus its own inherent advantages. The oscillatory part of the magnetoresistance can be isolated from the monotonic part and observed directly; where necessary, derivatives can be taken to emphasize the shorter periods; individual periods can be separated or eliminated by filtering; there is a large amount of data reduction in the recorded trace, and the periods can be averaged from the raw data. In addition, where narrow-banding (which is inherent in the derivative techniques) would be advantageous, the dc current source and amplifier can be replaced by an ac source and synchronous detection system.

Other applications

With the apparatus specific to the dHS measurements replaced by a pair of balanced mutual inductors, an ac source and lock-in amplifier, the above detecting and magnetic field apparatus was also used for observing the de Haas-van Alphen effect.[10]

Acknowledgments

I thank S. H. Koenig, who initiated this work, for his continued interest, Walter Schillinger for helpful discussion of the electronics and for the basic circuit for the coarse regulator, and R. N. Bhargava for experimental help and discussion of the results.

References

1. L. Shubnikov and W. J. de Haas, *Leiden Comm.* 207a, 107c, 207d, 210a (1930).
2. L. Onsager, *Phil. Mag.* **A250**, 325 (1952).
3. R. D. Brown, *Bull. Am. Phys. Soc.* **9**, 264 (1964).
4. S. H. Koenig (private communication).
5. S. Mase, S. von Molnar, and A. W. Lawson, *Phys. Rev.* **127**, 1030 (1962).
6. A. N. Friedman and S. H. Koenig, *IBM Journal* **4**, 158 (1960).
7. *Hall Generators*, Siemens and Halske Inc., Munich, Germany, 1959.
8. L. S. Lerner, *Phys. Rev.* **127**, 1480 (1962); *Phys. Rev.* **130**, 605 (1963).
9. J. B. Ketterson and Y. Eckstein, *Phys. Rev.* **132**, 1885 (1963); *Phys. Rev.* **137**, A1777 (1965).
10. R. N. Bhargava (to be published).

Received June 30, 1966